Pile Group Stiffness Computation and its Application in Ultra High-rise Buildings

Le calcul de raideur du groupe de piles et son application dans les immeubles ultra hauts

Weidong. Wang, Jiangbin. Wu, Adan. Wang
Arcplus Group PLC, Shanghai, China

ABSTRACT: In China, large pile groups are commonly used as deep foundations to support very heavily loaded ultra high-rise buildings. This paper presents some aspects of design and construction of Shanghai Centre Tower together with a brief description of liner elastic interaction factors of the large pile group. The issues of analysis of sheltering effect, reinforcing effect, group reinforcing effects, and group reinforcing coefficient are discussed with some theoretical calculations and engineering practice of large pile group. These will propose a new type of interaction factor being superimposed, established from subgroups of three pile, is introduced for floating group of piles of ultra high-rise building.

ABSTRAIT: En Chine, les grands groupes de pieux sont couramment utilisés comme des fondations profondes pour supporter des bâtiments très hauts et ultra chargés. Cet article présente certains aspects de la conception et de la construction de la Tour du Centre de Shanghai, ainsi qu'une brève description des facteurs d'interaction élastique de la doublure du groupe de grandes piles. Les questions d'analyse de l'effet d'abris, de l'effet de renforcement, des effets de renforcement du groupe et du coefficient de renforcement du groupe sont discutées avec quelques calculs théoriques et la pratique d'ingénierie du groupe de grandes masses. Ceux-ci proposeront un nouveau type de facteur d'interaction superposé, établi à partir de sous-groupes de trois pile, est introduit pour groupe flottant de piles de bâtiment ultra élevé.

KEYWORDS: large pile group; ultra high-rise building; sheltering effect; group reinforcing effects; group reinforcing coefficient

1 INTRODUCTION

With the rapid economic growth in the past two decades, numerous ultra high-rise buildings (UHRB) have been widely executed in Chinese riverside and coastal cities. According to statistics of Skyscraper City Report in 2012, the number of UHRB with height of more than 152 m will be more than 1300 in China during the next 10 years. Moreover, ten of them will be more than 600 m in height. UHRB, especially constructed in soft soil areas, have brought new challenges to geotechnical engineers. In order to satisfy sufficient bearing capacities and strict settlement control, large pile groups are often adopted for UHRB. As shown in Table 1, seven large groups of piles were designed for UHRB in Chinese riverside and coastal cities.

Table 1 A survey of pile foundations of some ultra high-rise buildings in China

Building name	Height (m)	Floors	Pile type	Pile diameter (mm)	Pile length (m)	Group size	Pile tip bearing stratum
Ping'an Finance Building	203.0	35	Bored pile	850	40.1	1235	Fine sand
Tianjin Tower	336.9	73	Bored pile	1000	60.0	351	Silty sand
Tianjin 117 Tower	597.0	117	Bored pile	1000	76.0	941	Silty sand
Shanghai Centre Tower	632.0	121	Bored pile	1000	51.0	955	Silty sand
SWFC	492.0	101	Steel pipe pile	700	60.7	1177	Medium coarse sand clipped in silt
Huamin Imperial Tower	258.0	60	Bored pile	800	57.0	417	Fine sand
Wuhan Center Tower	438.0	88	Bored pile	1000	46.1	448	Slightly weathered mud rock

In this type of foundation, numerous piles play an important role in settlement and different settlement reduction and support economical and safe design of the structure. Thus, accurately determining the pile settlement is critical. Analysis of pile group can be conducted in 2 ways: either accurately, using computer-based direct analysis of the whole group, or approximately, using superposition of interaction factors. Numerous former accurate numerical techniques such as the finite element method (FEM) and the boundary element method (BEM) have been used for pile settlement analysis (El Sharnouby & Novak, 1990; Sheil & McCabe, 2013). Typically, it needs a large amount of computer time for analysis with these numerical solutions. In order to improve efficiency, numerous approximate solutions based on the interaction factor method (IFM) have been presented to provide valuable insight and offer versatile design methods (Randolph & Wroth, 1978; Poulos & Davis, 1980; Mylonakis & Gazetas, 1998; Wang et al, 2016a, 2016b).

Unfortunately, some authors indicated that pile interaction effects may be overestimated by the analytical techniques based on linear elastic (LE) assumption (Poulos, 2001; McCabe & Sheil, 2015). Because the use of interaction factors based on LE soil parameters may overlook the potential soil modulus degradation occurs in the vicinity of pile. Therefore, numerous subsequent studies have shown that the nonlinear elastic behavior of single piles and small groups under vertical loading can be accurately and efficiently analyzed by recently simplified nonlinear elastic methods (Poulos, 1988; Huang et al, 2011; Mu et al, 2014). The literature features two alternatives for calculating two-pile interactive displacement: the passive pile may be loaded [henceforth referred to as Approach I; see Fig. 1(a)] or loaded free [henceforth referred to as Approach II; see Fig. 1(b) and Fig. 1(c)]. Predictions of the soil modulus at pile-soil interface of a designated passive pile determined using Approach I and II were compared and showed that for the range of parameters considered, Approach I showed satisfactory agreement to that predicted within groups. Approach II, however, consistently underpredicted the soil modulus at the pile-soil interface of the passive pile (McCabe & Sheil, 2015).

The concept of interaction factors illustrated by Poulos (1968) is very useful, particularly for small groups, but its applicability may suffer from a few drawbacks: the data of large groups published may not be quite accurate and the pile interaction effects may be overestimated (El Sharnouby & Novak, 1985). The latter inaccuracy may occur because the interaction factors being superimposed are calculated for any two-pile in group, ignoring the stiffening effect of intervening piles and thus disregarding the 'group reinforcing effects' (GRE) they have. Moreover, with increasing group size, this drawback generated by superposition cannot be neglected at all.

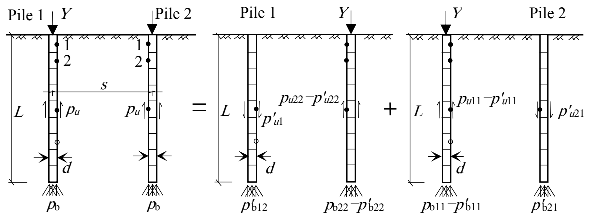

Fig. 1 (a) Approach I; (b) Approach II; (c) Approach II (in this study)

The purpose of this paper is to explore, using a new type of interaction factor being superimposed, the suitability of the IFM for estimating LE settlement of large floating groups, especially the foundation of UHRB. The analysis has two components:

- Based on loaded 'active' pile and unloaded 'passive' pile modeling, 'sheltering effect' (Mylonakis & Gazetas, 1998) and 'reinforcing effect' (Wang et al, 2016ab) of the passive pile can be deduced by Poulos IFM. To be applied to groups, the concept of 'group reinforcing coefficients' (GRC) is proposed to analyze GRE of large group. Comparison with Poulos IFM and Butterfield's BEM, the proposed IFM is verified simple in formulation and efficient in computation.
- Furthermore, this method is extended to analyze the response of the piled foundation of Shanghai Centre Tower. Arising from the limited soil layer assumption, pile interaction effects are analyzed by Poulos approximate IFM (Poulos & Davis 1980) and proposed IFM. Introducing the obtained piles stiffness into three dimensional (3D) FE model consists of raft and upper structure, the settlement of raft may be determined by using *ABAQUS* for this purpose. Interaction of the superstructure and real loading distribution are analyzed by 3D FE model in account into analyzing the behavior of foundation of Shanghai Centre Tower.

2 MEASURED SETTLEMENT OF PILED RAFT FOUNDATION OF SHANGHAI CENTRE TOWER

2.1 Soil parameters concerning Shanghai Centre Tower

In its construction site of the highest building in China, 632 m Shanghai Centre Tower in Shanghai Pudong Lujiazui financial centre (see Fig. 2), below a depth of 30 m from the ground, sand layers are encountered with a thickness of 60 m.

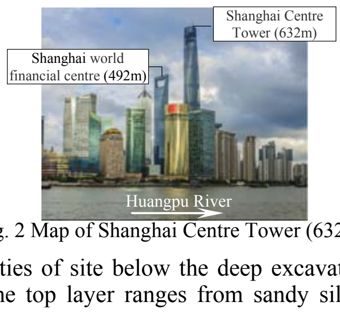

Fig. 2 Map of Shanghai Centre Tower (632 m)

Soil properties of site below the deep excavation are shown in table 2. The top layer ranges from sandy silt to fine sand, under the thick raft, with a thickness of about 40 m in general. Underlying are ⑨1 sandy silt, ⑨2-1 medium coarse sand clipped in silt, ⑨2-2 silt and ⑨3 fine sand with thickness of 7, 12, 11 and 4.8 m, respectively. The sandwich ⑨3t is silty clay with a thickness of 4.2 m. These ⑨3t silty clay and other sand layers are low to medium plastic and compressibility. Beneath the ninth layer are 7.2 m thick ⑩ stiff silty clay and 13.1 m thick ⑪ silt, respectively. The twelfth layer is silty clay with a thickness of 22 m. The sandwich ⑫1 is silt with a thickness of 4 m. Underlying the twelfth layer is silt with a thickness of bigger than 40 m. Soils above the tenth layer mainly consist of over-consolidated sand. The Young's modulus E_s of the seventh and ninth layers ranges 48~63 MPa. The E_s of the ⑦1 layer is small as 11.5 MPa. The seventh and ninth layers control the overall behavior of piled raft. The strength of soils below the ninth layer ranges 23.5~66 MPa. By contrast, the relatively constant poisson's ratio ν_s of all soil layers ranges from 0.20 to 0.30.

Table 2 Soil properties of site

Soil layer	Buried depth / m	Gravity Density γ/(kN/m^3)	Young's modulus E_s /MPa	Poisson ratio ν_s
⑦1 Silt clipped in Sandy silt	28.9−36.5	18.7	11.5	0.30
⑦2 Fine sand	64.7	19.2	48.0	0.25
⑦3 Silt	70.0	19.1	45.0	0.25
⑨1 Sandy silt	77.0	19.1	45.0	0.30
⑨2-1 Medium coarse sand	89.0	20.2	47.6	0.25
⑨2-2 Silt	100.0	19.3	44.5	0.25
⑨3 Fine sand	104.8	19.7	58.6	0.20
⑨3t Silty clay	109.0	19.1	34.6	0.35
⑨3 Fine sand	125.7	19.7	62.3	0.20
⑩ Silty clay	132.9	19.3	23.5	0.35
⑪ Silt	146.0	19.0	41.6	0.30
⑫ Silty clay	159.0	20.0	36.9	0.20
⑫1 Silt	163.0	19.5	31.3	0.25
⑫ Silty clay	172.0	19.0	40.8	0.30
⑬ Silt	212.7	19.1	66.0	0.25

2.2 Measured settlement of piled raft foundation

The accuracy of proposed IFM for analysis of piled foundation is further verified by comparing with the monitoring data of raft under Shanghai Centre Tower, which is founded on 955 large-diameter super-long bored piles. The building has 121-layer superstructure and 5-story basements from street. Embedded depth of raft rises 31.4 m from the ground and its thickness is about 6 m. The piles are designed to be with diameter d=1 m, length L=88 m from the ground (effective length L_e=51.2 m down from raft), Young's modulus E_p=3.35×10^7 kPa and cross-sectional coefficient of 1. Fig. 3 shows that all piles are located in a large octagon. Quincunx laying-out piles are located in concentrated load range under core-wall structure and huge columns. Other piles are located in shape of orthogonal frame. The monitoring raft settlement is also shown in this figure.

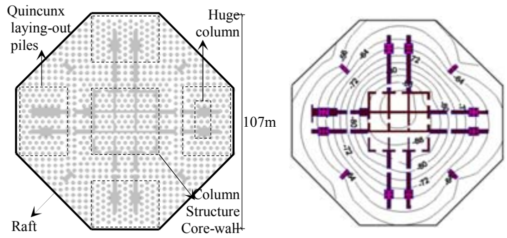

Fig. 3 Location of the piles and monitoring result (S_{max}: 93 mm)

3 POULOS INTERACTION FACTOR METHOD

Poulos (1968) defined the interaction factor α as

$$\alpha_{ij} = W_{ij} / W_{ii} \quad (1)$$

where α_{ij} = interaction factor for pile i due to a loaded pile j in group, corresponding to the center-to-center spacing (s) between piles i and j; W_{ii} = settlement of pile i when loaded alone (by vertical static load P_i), i.e., a single pile; and W_{ij} = additional settlement of pile i caused by load P_j acting on nearby pile j.

The value of W_{ij} in Eq. (1) can be calculated using Approach I and II as detailed in the following sections. (a) Approach I:

For each value of s/d, W_{ij} is determined, assuming pile i is loaded [i=1, j=2, see Fig. 1(a)], and the corresponding value of α_{ij} is calculated. In which, d is the diameter of a circular pile or an equivalent diameter of a noncircular pile. In this case, the relative shear stress at pile-soil interface of pile j is relatively small, and therefore there is no soil modulus degradation at pile j. (b) Approach II: For each value of s/d, W_{ij} is determined, assuming pile i is not loaded [i=1, j=2, see Fig. 1(c)], and the corresponding value of α_{ij} is calculated.

The calculation of settlement, W_i of a pile i in a n-pile group by the Poulos IFM may be obtained using (Poulos 2006),

$$W_i = \sum_{j=1}^{n} (P_j W_1 \alpha_{ij}) \tag{2}$$

where P_j = load on pile j; W_1 = settlement of single pile per unit load (= W_{ii} / P_i); n = group size.

4 SHEILTERING-REINFORCING EFFECT

In order to analyze GRE of pile group effectively, sheltering effect and reinforcing effect would be deduced, respectively. The method described in Fig. 1(a) is described by Poulos (1968) for floating groups. Two identically loaded piles is considered, as shown in Fig. 1(a), and as with the single-pile analysis, two piles are respectively divided into n_1 and n_2 cylindrical elements and a uniformly-loaded circular base. If conditions remain purely elastic in soil and no slip occurs at the pile-soil interface, the pile-soil displacements of each element may be equated as,

$$\boldsymbol{U}_v = \frac{d}{E_s}(\mathrm{I}_{v1} + \mathrm{I}_{v2})\,\boldsymbol{p} \tag{3}$$

where $\boldsymbol{U}_v$ is vector of v-soil displacement; $\boldsymbol{p}$ denotes n_1+n_2+2 shear stress vector; I_{v1}+I_{v2} stands for (n_1+n_2+2)(n_1+n_2+2) matrix of displacement influence factors, which is matrix at element v on pile 1 by shear stress on element u of two piles, respectively.

In LE soil layer, Fig. 1 shows that Approach I is strictly equal to two Approach II. As an example, in Fig. 1(c), p_{u11} is shear stress of a single-pile under vertical load Y; $p_{u11}-p'_{u11}$ is shear stress considering reinforcing effect on pile 1; p'_{u21} is shear stress considering sheltering effect from pile 2 itself. Similarly, $p_{b11}-p'_{b11}$ is tip resistance of pile 1 and p'_{b21} is tip resistance.

The calculation of pile-side soil free-field displacement, U_{11} and U_{21}, of pile 1 and pile 2 in a two-pile group like Fig. 1(c) by Approach II may be obtained using the following formula,

$$\begin{Bmatrix} U_{11} \\ U_{21} \end{Bmatrix} = \begin{Bmatrix} [F_s]_{11} & [F_s]_{12} \\ [F_s]_{21} & [F_s]_{22} \end{Bmatrix} \begin{Bmatrix} p_{11} \\ p_{21} - p'_{21} \end{Bmatrix} \tag{4}$$

where $[F_s]_{11}$ and $[F_s]_{22}$ are identical with $d\mathrm{I}_{11}/E_s$ and $d\mathrm{I}_{22}/E_s$ square matrix, respectively; $[F_s]_{21}$ and $[F_s]_{12}$ stand for $d\mathrm{I}_{21}/E_s$ and $d\mathrm{I}_{12}/E_s$ matrix, respectively; p_{11} is shear stress of a single-pile under vertical load; p_{21} is shear stress un-considering pile 2; p'_{21} is shear stress considering the sheltering effect of pile 2.

When purely elastic conditions prevail at pile-side interface, the displacements of adjacent points along the interface are equal, $\{W\}$=$\{U\}$. This modified pile displacement considering passive pile stiffness may be given by Eq. (4), as follows:

$$\begin{aligned} \{W_{11}\} &= [F_s]_{11} \cdot \{p_{11}\} + [F_s]_{12} \cdot \{p_{21} - p'_{21}\}; \\ \{W_{21}\} &= [F_s]_{21} \cdot \{p_{11}\} + [F_s]_{22} \cdot \{p_{21} - p'_{21}\} \end{aligned} \tag{5}$$

where $[F_s]_{22}\cdot\{p_{21}-p'_{21}\}$ and $[F_s]_{12}\cdot\{p_{21}-p'_{21}\}$ stand for the sheltering effect of passive pile 2 and the reinforcing effect on active pile 1 arising from pile 2, respectively.

5 A NEW IFM OF LARGE PILE GROUP

5.1 Three-pile model

Comparison with sheltering effect, reinforcing effect can be completely neglected in two-pile interaction factors (see Fig. 4). However, other numerous intervening piles may follow this potential reinforcing effect, which may be overlooked by the use of interaction factors based solely on the spacing of any pair of piles in a group. To this end, we propose a new type of interaction factor involving three consecutive steps to reasonably compute the GRE of three-pile group.

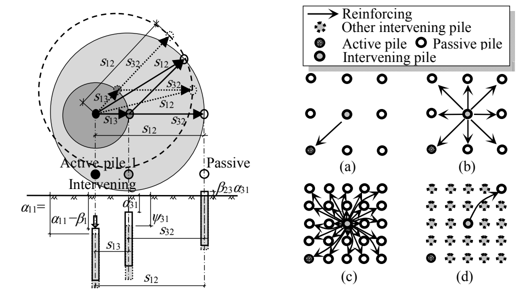

Fig.4. GRE of intervening pile introduced by three-pile model and when loaded on the corner pile, (a) reinforcing effect from center intervening pile in 9-pile group, (b-c) overall GRE from center intervening pile in 9 and 25 pile groups and (d) GRE on the corner passive pile from center intervening pile, influenced by other intervening piles in 25-pile group

Step 1. The active pile 1 is subjected to a vertical load at its head. The unit settlement profile $W_{11}(0)$ atop the pile can be determined by Poulos single-pile analysis or other methods.

Step 2. Based on approach II, the presence of intervening pile 3 reduces the soil free-field displacement generated by active pile 1. For a soil profile consisting of homogeneous horizontal layer, it is assumed that the attenuation of soil settlement with radial distance from pile 3 can be modified by the matrix variation of Eq. (5). At the location of pile 3 in Fig. 2, if pile 3 were not present, the soil settlement would be as ψ_{31} based on Mindlin displacement equation. However, the stiffness of pile 3 reduces the above settlement as α_{31} ($<\psi_{31}$). Extending this sheltering effect of pile 3, one can determine the reinforcing effect $\alpha_{31}\beta_{13}$ from pile 3 to pile 1. Thus, if these two piles were present, the settlement would be respectively obtained by,

$$W'_{11}(0) = W_{11}(0)(\alpha_{11} - \beta_{13}\alpha_{31});\ W_{31}(0) = W_{11}(0)\alpha_{31} \tag{8}$$

Step 3. This reinforcing effect on soil free-field displacement from intervening pile 3 may not only reduce the settlement of active pile 1 but also reduce the settlement of passive pile 2 (see Fig. 4). Extending Approach II, additional displacement of any soil point arising from all segments divided by overall three piles may be calculated by simultaneous analysis based on Mindlin displacement solution. The calculation result shows that the interaction factor between any two piles may be modified by the potential reinforcing effect of intervening pile. As an example in Fig. 4, when loaded on pile 1, the GRE $\beta_{23}\alpha_{31}$ on passive pile 2 from intervening pile 3 reduces two-pile interaction factor α_{21} based on loaded active pile 1 and unloaded passive pile 2. The modified additional settlement of pile 2 is

$$W_{21}(0) = W_{11}(0)(\alpha_{21} - \beta_{23}\alpha_{31}) \tag{9}$$

When loaded on the corner pile, Fig. 4(a, b) reminds that two-pile reinforcing effect is just a small part of the GRE to account for the stiffness of the center intervening pile. As an example in Fig. 4(a, c), the GRE on any passive pile arising from the center intervening pile in small groups (e.g. 3×3, 5×5 piles) may be calculated by superimposing the GRE of any three piles (i.e. any active pile - the center intervening pile - any passive pile) in the group. Therefore, the additional settlement $W_{i,\mathrm{GRE}}$ of passive pile i within n-pile group may be obtained by:

$$W_{i,\mathrm{GRE}} = \sum_{j=1}^{n} \Big(P_j W_1 \sum_{k=1}^{n,\neq j} \alpha_{kj}\beta_{ik}\Big) \qquad (\beta_{ii} = 0) \tag{10}$$

where, when loaded on pile j, $\alpha_{kj}\beta_{ik}$ is the GRE on passive pile i arising from intervening pile k.

This method is varied in less than 49-pile group based on shearing displacement method (Wang et al, 2016ab). For larger groups, however, the overall GRE being superimposed may not be of sufficient accuracy based on three-pile model, which may overlook the potential effects of other numerous intervening piles (see Fig. 4(d)). Thus, the GRE in large groups would be discussed and modified further, especially large group of UHRB.

5.2 Group reinforcing coefficient

In order to consider the effect of other intervening piles, GRC (less than reinforcing coefficient) is deduced in this study. As an example, when loaded solely on pile 1 in a 4-pile group, the reinforcing coefficient β_{12} between pile 1 and intervening pile 2 may be modified as $\beta_{12}-\beta_{32}\beta_{13}-\beta_{42}\beta_{14}$ by considering the effect of other intervening piles 3, 4. Similarly, $\beta_{32}\beta_{13}$ and $\beta_{42}\beta_{14}$ can be further modified as $(\beta_{32}-\beta_{42}\beta_{34})(\beta_{13}-\beta_{43}\beta_{14})$ and $(\beta_{42}-\beta_{32}\beta_{43})(\beta_{14}-\beta_{34}\beta_{13})$ using the intervening pile 4 and pile 3. Thus, the GRC between pile 1 and pile 2 may be finally obtained as $\beta_{12}-(\beta_{32}-\beta_{42}\beta_{34})\times(\beta_{13}-\beta_{43}\beta_{14})-(\beta_{42}-\beta_{32}\beta_{43})\times(\beta_{14}-\beta_{34}\beta_{13})$.

Similarly, for *n*-pile group, a general expression obtained for the GRC may be used to analyze the total modified interaction factors for large pile group, described as,

$$\begin{bmatrix} 1 & \cdots & \beta_{1j}-\sum_{u=1}^{n,u\neq 1,j}\left[\beta_{uj}-\sum_{v=1}^{n,v\neq 1,j,u}(\beta_{vj}-\cdots)(\beta_{uv}-\cdots)\right]\cdot\left[\beta_{1u}-\sum_{v=1}^{n,v\neq 1,j,u}(\beta_{vu}-\cdots)(\beta_{1v}-\cdots)\right] & \cdots & \beta_{1n}-\sum_{u=1}^{n,u\neq 1,n}\left[\beta_{un}-\sum_{v=1}^{n,v\neq 1,n,u}(\beta_{vn}-\cdots)(\beta_{uv}-\cdots)\right]\cdot\left[\beta_{1u}-\sum_{v=1}^{n,v\neq 1,n,u}(\beta_{vu}-\cdots)(\beta_{1v}-\cdots)\right] \\ \vdots & \ddots & \vdots & ⋰ & \vdots \\ \beta_{i1}-\sum_{u=1}^{n,u\neq i,1}\left[\beta_{u1}-\sum_{v=1}^{n,v\neq i,1,u}(\beta_{v1}-\cdots)(\beta_{uv}-\cdots)\right]\cdot\left[\beta_{iu}-\sum_{u=1}^{n,u\neq i,1,u}(\beta_{vu}-\cdots)(\beta_{iv}-\cdots)\right] & \cdots & 1 & \cdots & \beta_{in}-\sum_{u=1}^{n,u\neq i,n}\left[\beta_{un}-\sum_{v=1}^{n,v\neq i,n,u}(\beta_{vn}-\cdots)(\beta_{uv}-\cdots)\right]\cdot\left[\beta_{iu}-\sum_{u=1}^{n,u\neq i,n,u}(\beta_{vu}-\cdots)(\beta_{iv}-\cdots)\right] \\ \vdots & ⋰ & \vdots & \ddots & \vdots \\ \beta_{n1}-\sum_{u=1}^{n,u\neq n,1}\left[\beta_{u1}-\sum_{v=1}^{n,v\neq n,1,u}(\beta_{v1}-\cdots)(\beta_{uv}-\cdots)\right]\cdot\left[\beta_{nu}-\sum_{u=1}^{n,u\neq n,1,u}(\beta_{vu}-\cdots)(\beta_{nv}-\cdots)\right] & \cdots & \beta_{nj}-\sum_{u=1}^{n,u\neq n,j}\left[\beta_{uj}-\sum_{v=1}^{n,v\neq n,j,u}(\beta_{vj}-\cdots)(\beta_{uv}-\cdots)\right]\cdot\left[\beta_{nu}-\sum_{u=1}^{n,u\neq n,j,u}(\beta_{vu}-\cdots)(\beta_{nv}-\cdots)\right] & \cdots & 1 \end{bmatrix} \begin{bmatrix} \alpha'_{11} \\ \vdots \\ \alpha'_{jj} \\ \vdots \\ \alpha'_{nn} \end{bmatrix}_k = \begin{bmatrix} \alpha_{1k} \\ \vdots \\ \alpha_{jk} \\ \vdots \\ \alpha_{nk} \end{bmatrix}$$

$$\left[\alpha'_{11}\,\alpha'_{22}\cdots\alpha'_{jj}\cdots\alpha'_{nn}\right]^{\mathrm{T}}=\sum_{k=1}^{n}\left[\alpha'_{11}\,\alpha'_{22}\cdots\alpha'_{jj}\cdots\alpha'_{nn}\right]_k^{\mathrm{T}};\alpha_{jj}=1 \qquad (i=1,2,\cdots,n,\ j=1,2,\cdots,n,\ k=1,2,\cdots,n) \tag{11}$$

where, loaded on pile *k*, pile *j* isintervening pile; pile *i* is passive pile; $[\alpha'_{ii}]_k$ is unknown settlement coefficient matrix of pile *i*.

6 APPLICABILITY TO SHANGHAI CENTRE TOWER

6.1 FE modeling of Shanghai Centre Tower

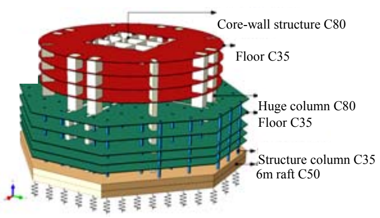

Fig. 5 3D FE model of the piled foundation

The authors used *ABUQUS* 6.10 in conjunction with the LE soil model for this purpose. Note that total 3D FE model of the pile-soil-raft-structure is too complex and time consuming to be developed. To analyze the rigidity interaction of superstructure and thick raft, this model comprises the thick raft, basements, superstructures, core-wall, floor structure, huge mega-frame columns and numerous structure columns. The geometry of the S4R shell-model elements are employed to represent the raft and floor structure analyzed. Structure columns, core-wall and huge mega-frame columns are modeled as 3D solid model with C3D8R element type. The total finite elements number of the 3D FE model is about 900,000.

6.2 Settlement for piled foundation of Shanghai Centre Tower

The stiffness of pile springs is obtained under the average load (6293 kN) which is equal to the ratio of the total load and pile numbers. Referencing the solid pier foundation method, there may be a concept of the existence of a static surface on which the additional stress is equal to about 10% of gravity stress. Thus, using this stress ratio, when two-pile interaction factor is analyzed based on assumed limited layer (Poulos & Davis, 1980), the settlement of piled foundation is shown in Fig.6. Although the calculation result and the monitoring result are only approximately comparable. The accuracy (or not) of the soil E_s will influence settlement prediction. Nevertheless, the agreement between these results is satisfactory: S_{max}=128mm, S_{diff}=71mm and S_{max}=111mm, S_{diff}=41mm (see Fig. 6 and Fig. 3) with FEM solution based on the proposed IFM and the measure result, respectively. While, FEM result based on Poulos IFM is excessively exaggerated as S_{max}=216 mm, S_{diff}=120 mm.

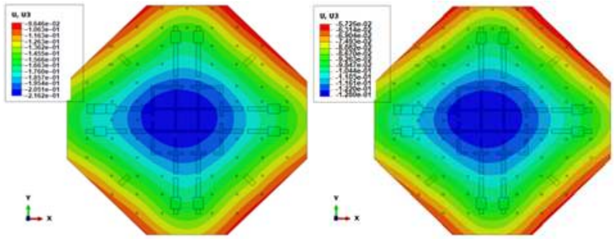

(d) FEM solution based on Poulos IFM (unit: mm) (e) FEM solution based on proposed IFM (unit: mm)

Fig. 6 Contour map of settlement in limited soil layer assumption

7 CONCLUSIONS

It is believed that the results of this paper complement and extend the seminal work on the topic by Wang et al (2016ab). A simple physical method has been presented for calculating the interaction factors and settlement of large group. The basis of the method is a generalized LE model for pile-pile interaction analysis. To solve the overestimate settlement by superimposing two-pile interaction factor, GRE of numerous intervening piles in a group is analyzed based on the proposed GRC. Extensive comparisons with available monitoring settlement results of the piled raft foundation of Shanghai Centre Tower confirmed the validity of the proposed IFM used to large group of UHRB.

REFERENCES

El Sharnouby, B., and Novak, M. (1990). “Stiffness constants and interaction factors for vertical response of pile groups.” Can. Geotech. J., 27(6), 813-822.

Sheil, B.B. and McCabe, B.A. (2013). “A finite element based approach for predictions of rigid pile group stiffness efficiency in clays.” Acta Geotechnica, 9(3):469-484.

Randolph, M.F. and Wroth, C.P. (1978). “Analysis of deformation of vertically loaded piles.” J. Geotech. Eng., 104(12), 1465-1488.

Poulos, H.G. and Davis, E.H. (1980). “Pile foundation analysis and design.” John Wiley and Sons, New York.

Mylonakis, G. and Ggazetas, G. (1998). “Settlement and additional internal forces of grouped piles in layered soil.” Géotechnique, 48(1), 55-72.

Wang, A.D., Wang, W.D., Huang, M.S., and Wu, J.B. (2016a). “Interaction factor for large pile groups.” Géotech. Lett., 6(1), 1-8.

Wang, A.D., Wang, W.D., Huang, M.S., and et al. (2016b). “Discussion: Interaction factor for large pile groups.” Géotech. Lett., 6(1), 1-7.

Poulos, H.G. (2001). “Piled raft foundations: design and applications.” Géotechnique, 51(2), 95-113.

McCabe, B.A. and Sheil, B.B. (2015). “Pile group settlement estimation: suitability of nonlinear interaction factors.” Int. J. Geomech., 15(3), 04014056.

Poulos, H.G. (1988). “Modified calculation of pile group settlement interaction.” J. Geotech. Eng., 114(6), 697-706.

Huang, M.S., Liang, F.Y. and Jiang, J. (2011). “A simplified nonlinear analysis method for piled raft foundation in layered soils under vertical loading.” Comput. Geotech., 38(7), 875-882.

Mu, L.L., Huang, M.S. and Lian, K.N. (2014). “Analysis of pile-raft foundations under complex loads in layered soils.” Int. J. Numer. Anal. Meth. Geomech., 38(38), 256-280.

Poulos, H.G. (1968). “Analysis of the settlement of pile groups.” Géotechnique, 18(1), 449-471.

El Sharnouby, B., and Novak, M. (1985). “Static and low frequency response of pile groups.” Can. Geotech. J., 22(22), 79-94.

Poulos, H. G. (2006). “Pile group settlement estimation—Research to practice.” Proc., GeoShanghai Int. Conf. on Foundation Analysis and Design: Innovative Methods, R. L. Parsons, L. Zhang, W. D. Guo, K. K. Phoon, and M. Yang, eds., ASCE, Reston, VA, 1–22.